In Situ Investigation of the Nature of the Active Surface of a Vanadyl Pyrophosphate Catalyst during *n*-Butane Oxidation to Maleic Anhydride

M. Hävecker,*,† R. W. Mayer,†,|| A. Knop-Gericke,† H. Bluhm,† E. Kleimenov,† A. Liskowski,† D. Su,† R. Follath,§ F. G. Requejo,⊥,‡ D. F. Ogletree,⊥ M. Salmeron,⊥ J. A. Lopez-Sanchez,# J. K. Bartley,# G. J. Hutchings,# and R. Schlögl†

Fritz-Haber-Institut der Max-Planck-Gesellschaft, Department of Inorganic Chemistry, Faradayweg 4-6, D-14195 Berlin, Germany, Department of Chemistry, Cardiff University, P. O. Box 912, Cardiff CF10 3TB, United Kingdom, Berliner Elektronenspeicherringgesellschaft für Synchrotronstrahlung (BESSY), Albert-Einstein-Strasse 15, D-12489 Berlin, Germany, and Lawrence Berkeley National Laboratory, Materials Science Division, Berkeley, California 94720

Received: October 21, 2002; In Final Form: January 26, 2003

In situ X-ray absorption spectroscopy (XAS) and in situ X-ray photoelectron spectroscopy (XPS) have been applied to study the active surface of vanadium phosphorus oxide (VPO) catalysts in the course of the oxidation of *n*-butane to maleic anhydride (MA). The V L_3 near edge X-ray absorption fine structure (NEXAFS) of VPO is related to the details of the bonding between the central vanadium atom and the surrounding oxygen atoms. Reversible changes of the NEXAFS were observed when going from room temperature to the reaction conditions. These changes are interpreted as dynamic rearrangements of the VPO surface, and the structural rearrangements are related to the catalytic activity of the material that was verified by proton-transfer reaction mass spectrometry (PTR-MS). The physical origin of the variation of the NEXAFS is discussed and a tentative assignment to specific V−O bonds in the VPO structure is given. In situ XPS investigations were used to elucidate the surface electronic conductivity and to probe the ground state of the NEXAFS spectra.

Introduction

Vanadium phosphorus oxide (VPO) catalysts that contain as the main crystalline phase vanadyl pyrophosphate $(VO)_2P_2O_7$ are well-known for the mild oxidation of the inert alkane *n*-butane to maleic anhydride (MA).[1] MA is an important intermediate for polyester resin production. Many reviews have appeared about this material in the past decade, while extensive scientific work has been performed to optimize the preparation, activation, and catalytic conditions and to understand the peculiar properties of VPO.[2−7] Nevertheless, the nature of the active sites of this catalyst is still a matter of debate. In addition to its industrial relevance, VPO is a very interesting material because it can selectively catalyze the oxidation of several hydrocarbons. This is unusual since most other catalysts are specific to just a single reaction. Furthermore, only VPO and V_2O_{5-x} supported by TiO_2-anatase are selective in the oxidation of *n*-butane to maleic anhydride. This is a very demanding reaction in the sense that it necessitates the abstraction of eight H atoms, incorporation of three oxygen atoms into the *n*-butane molecule, and the transfer of 14 electrons within the solid to ensure the redox Mars and van Krevelen mechanism to occur[8,9] corresponding to

$$CH_3\text{-}CH_2\text{-}CH_2\text{-}CH_3 + 7O \rightarrow C_4H_2O_3 + 4H_2O$$

There are various explanations for the reaction mechanism of the *n*-butane oxidation to MA. Most authors believe that the reaction proceeds via a consecutive alkenyl mechanism.[10] The proposed intermediate products of the oxidation are 1-butene, 1-3 butadiene, dihydrofuran, and furan before the ultimate formation of MA. Several alternative mechanisms have also been proposed.[8,11−12]

The chemistry of vanadium oxides is particularly rich and leads to compounds with very interesting physical and chemical properties.[13] A variety of vanadium ions in different formal valences exist and a broad range of electric and magnetic properties are shown by these materials. The preparation and long-term activation of VPO catalysts have been the subject of extensive studies.[14] It is clear that the surface chemistry and the bulk properties of the active catalyst change with the time of activation.[4,15] The evolution of the catalyst in the course of the activation process goes along with an evolution of the catalyst performance. Its surface structure is dependent on the activation conditions.

The composition of the VPO surface is complex since crystalline phases other than the main phase vanadyl pyrophosphate are often observed and disordered phases are also found.[16−18] Actually, Hutchings et al. have recently shown the potential of completely amorphous VPO catalysts.[19] Some authors state that vanadyl pyrophosphate is the sole catalytically active phase,[20,21] while others believe that the active site in VPO catalysts is a combination of vanadyl pyrophosphate along with patches of $VOPO_4$ polymorphs or isolated V^{5+} centers on the surface of a $(VO)_2P_2O_7$ core.[17,22] The significance of defects,

* To whom correspondence should be addressed. Tel: +49 30 8413 4422. Fax: +49 30 8413 4677. E-mail: mh@fhi-berlin.mpg.de.
† Fritz-Haber-Institut der Max-Planck-Gesellschaft.
# Cardiff University.
§ Berliner Elektronenspeicherringgesellschaft für Synchrotronstrahlung (BESSY).
⊥ Lawrence Berkeley National Laboratory.
|| Present address: Degussa, Project House Catalysis, Industriepark Höchst, D-65926 Frankfurt/M, Germany.
‡ Fellow of CONICET, Argentina.

10.1021/jp027259j CCC: $25.00
Published on Web 04/15/2003

for example, shear steps formed on the surface of $(VO)_2P_2O_7$ upon exposure of the catalyst to *n*-butane, has been recognized.[23]

From the discussion above, it becomes evident that the real nature of the active sites of the VPO catalyst is still a matter of debate. The capability of the VPO system to form many different phases with similar structures often leads to a multiphase system. The complexity of the VPO system is enhanced by the fact that all these phases can be transformed easily into each other. The different phases can affect the catalyst's performance in various ways.

In this work, we used in situ X-ray photoelectron spectroscopy (XPS) and in situ X-ray absorption spectroscopy (XAS). XPS can be used to obtain information about the surface oxidation state by analyzing the O1s and V2p peaks. The detected photoelectrons of the O1s and V2p core levels had a kinetic energy of 200 eV resulting in a probing depth of approximately 1 nm for this method.[24] XAS in the soft energy range, the method mainly applied in this work, is especially suitable to contribute to the understanding of the VPO system. This technique is not restricted to crystalline phases but is well suited to study materials without any long range order because X-ray absorption spectroscopy is a local method. Both ordered and disordered phases are accessible. Furthermore, XAS is surface sensitive when applied in the electron yield mode in the soft energy range. The probing depth of this method can be estimated to be about 4 nm.[25] Thus, the important surface and near surface layers of the catalyst can be studied. Another point in the case of the VPO V L_3 NEXAFS is the feasibility to deconvolute at least qualitatively the overall spectral function at the absorption edge into regimes with main contributions from singly coordinated oxygen, doubly coordinated oxygen, and triply coordinated oxygen, respectively.[26] Hence, it becomes possible to get spectroscopic information about specific V−O bonds. Finally, XAS in the soft energy range can be applied in situ to study the relevant electronic surface structure of the catalyst under working conditions. Thus, this technique is in particular valuable to study the active phase of this highly relevant catalytic system. Hence, in this paper we present a detailed study of the surface of a VPO catalyst.

Experimental Details

Catalyst Preparation and Testing. Vanadium phosphate catalyst precursors were prepared using pyrophosphoric and phosphorous acid as a reducing agent as follows. V_2O_5 (5.9 g, Strem, 99%), $H_4P_2O_7$ (1.703 g, Aldrich, 99%), and H_3PO_3 (4.1 g, Aldrich, 99%) were mixed with distilled water (20 mL) and heated in an autoclave (145 °C, 72 h). Following the reaction, the solid produced was recovered by filtration, washed with cold distilled water (50 mL), and dried in air (120 °C, 16 h). The precursors were refluxed with distilled water (20 mL/g of solid) for 2 h. The solid was recovered by filtration when hot, washed with distilled water (50 mL), and dried in air.

The catalyst was tested under usual conditions prior to the XAS experiments using a microreactor with a standard mass of catalyst (0.5 g). Air and *n*-butane were fed to the reactor via calibrated mass flow controllers to give a feedstock composition of 1.7% *n*-butane in air (GSHV: 2477 h^{-1}). The products were then fed via heated lines to an on-line gas chromatograph for product analysis. The reactor comprised a stainless steel tube with the catalyst held in place by plugs of quartz wool. A thermocouple was located in the center of the catalyst bed and temperature control was typically better than ± 1 °C. Carbon mass balances of ≥97% were typically observed. Catalyst precursors were heated in situ (1.8% *n*-butane in air) at 400 °C by heating the sample from room temperature at a rate of 3 °C/min. After 56 h of activation a selectivity of 57% to MA at a *n*-butane conversion of 63% was obtained.

X-ray Absorption Spectroscopy Experiments. After testing the catalyst in the microreactor the catalyst powder (50 mg) was pressed into a self-supporting flat pellet (diameter 13 mm) and fixed on a stainless steel sample holder for further characterization by in situ X-ray absorption spectroscopy. The XAS experiments were performed using a special reactor cell designed for in situ X-ray absorption investigation. Details about the setup and the data processing can be found in the literature.[27−29] For the in situ experiments, a continuous flow of 1.5 vol % *n*-butane in He balance and oxygen were dosed via two calibrated mass flow controllers at a total mass flow of 17.5 sccm. The partial pressures of the *n*-C_4H_{10}/He mixture and the oxygen were 1.6 and 0.4 mbar, respectively, resulting in a total pressure in the reactor of 2 mbar during the XAS measurements. The sample was heated in the reaction mixture up to 400 °C by a resistive heater at a rate of 20 °C/min. The sample temperature was held at 400 °C for typically 120 min and then decreased again. Part of the gas outlet from the XAS cell was fed into a proton-transfer-reaction mass spectrometer (PTR-MS, IONICON ANALYTIK) used for reaction product analysis. This system is based on the principle of chemical ionization using H_3O^+ as the proton donator combined with the swarm technique of the flow tube type. It is especially suitable for a qualitative and quantitative product analysis at ppb level.[30,31]

The gas from the reactor was diluted with air passed into the mass spectrometer via a carbon filter to avoid gas discharge in the drift tube of the instrument due to the large He content in the gas phase in the XAS reactor. He was chosen as balance for the XAS experiments because of its low photon absorption coefficient and its low cross section for inelastic electron scattering, which makes it especially suitable for electron spectroscopy in the soft energy range.

Experiments were carried out at the undulator beamline U/49-2 at the third generation synchrotron radiation facility BESSY in Berlin.[32,33] Vanadium L_3-edge spectra were normalized to the same maximum peak height and analyzed by a least-squares fit, using Gauss-Lorentz profiles considering experimental and intrinsic broadening. The data were collected in situ in the total electron yield mode (TEY) under gas flow conditions at a total pressure of 2 mbar. The photon energy of the NEXAFS spectra was calibrated by the π^*-resonance of molecular oxygen at 530.8 eV.[34] The resolving power $E/\Delta E$ was about 5000.

X-ray Photoelectron Spectroscopy Experiments. In situ XPS experiments were performed at beamline 9.3.2 at the Advanced Light Source (ALS) in Berkeley.[35] Details of the experimental setup can be found in Ogletree et al.[36] A photon energy of $h\nu = 720$ eV was chosen for excitation of the O1s and V2p core levels. The spectral resolving power of the beamline $E/\Delta E$ was about 1000. The pass energy of the hemispherical analyzer was set to 11.75 eV.

The same sample pellet was used for the in situ XPS study as for the in situ XAS experiments described above. Furthermore, the same gas mixture of *n*-butane, oxygen, and helium at the same total pressure of 2 mbar was applied. A continuous flow of 1.5 vol % *n*-butane in He balance and oxygen were dosed via two calibrated mass flow controllers at a total mass flow of 11 sccm.

Product gas analysis was carried out with a conventional electron-impact mass spectrometer mounted in the third differential pumping stage of the in situ XPS chamber. This was

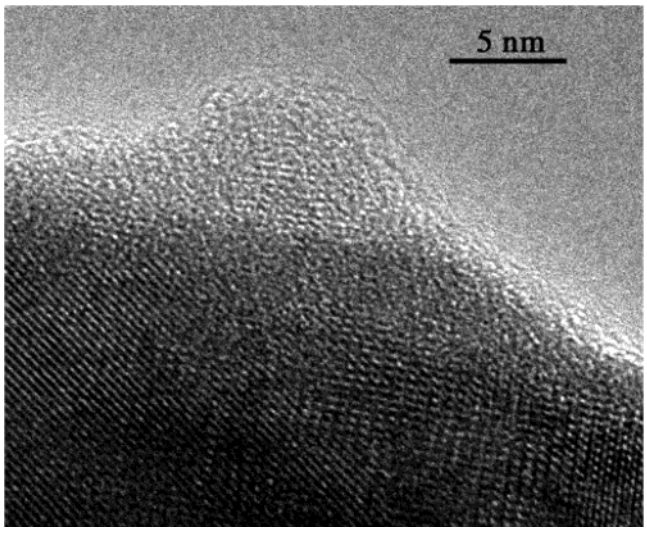

Figure 1. High-resolution TEM micrograph of a VPO catalyst particle. The image reveals the disordered surface on the well-crystallized particles.

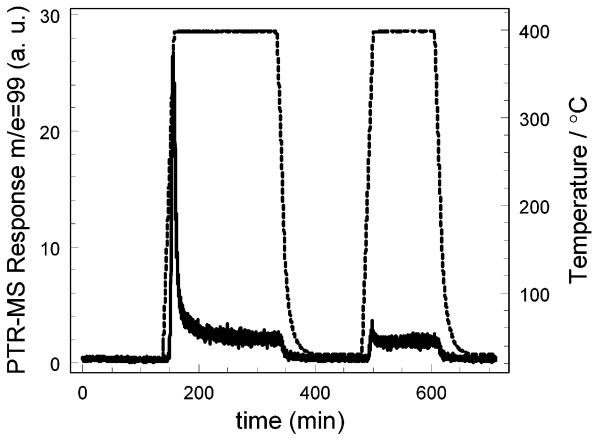

Figure 2. PTR-MS response signal (solid line) for maleic anhydride ($m/e = 99$) while the catalyst was heated from room temperature to 400 °C and cooled to room temperature twice in a mixture of n-C_4H_{10}/O_2 and He (1.2 vol %/20 vol %/78.8 vol %). The temperature of the catalyst is indicated by the dashed line. It can be seen clearly that the catalyst is active for maleic anhydride when it reaches the reaction temperature.

much less sensitive than the directly coupled PTR-MS used in the XAS experiments. The same reaction conditions were established during the XPS study as in the XAS experiments. Thus, it can be assumed that the sample pellet showed the same catalytic performance as in the X-ray absorption experiment, although no reactant conversion could be unequivocally identified.

Results and Discussion

Several authors suggest that the active phase is more complex than the simple $(VO)_2P_2O_7$ model. This idea is supported by XPS investigation of the surface of VPO catalysts. Usually a P/V ratio greater than 1 and an oxidation state slightly larger than 4.0 are found. A P/V ratio of 1.2 and an average vanadium valence of +4.2 was found for the catalyst material used for the in situ studies reported here by ex situ XPS studies. The composition of the VPO surface is complex because not only other crystalline phases than the main phase vanadyl pyrophosphate are often observed but also disordered phases were found.[16−18] HRTEM investigations of the catalyst that is used in this paper also revealed the existence of a disordered layer at the surface. A TEM micrograph of the material is displayed in Figure 1. It was taken with a Philips CM 200 FEG transmission microscope operated at 200 kV. Figure 1 shows that there is a disordered layer at the surface of the well-ordered crystalline vanadyl pyrophosphate bulk.

These findings stress the importance of the application of surface sensitive techniques such as in situ XAS and in situ XPS. Furthermore, it was found that only the surface and near surface layers take part in the reaction.[37] In the fresh catalysts, lattice oxygen is very easily lost due to defects in the VPO structure, while with an equilibrated catalyst, lattice oxygen is not as labile. The participating lattice oxygen belongs to only a few surface layers, about 4.

Reaction Product Analysis. In situ characterization of catalysts by spectroscopic methods demands a verification of the catalytic activity of the material under investigation in the same setup used for the spectroscopic characterization at the actually applied conditions. This actually might be different to that determined in a microreactor where the catalyst was tested for its catalytic characterization. The same catalyst material and a similar reactant gas mixture were used for the XAS investigation and for the catalytic test carried out prior in the microreactor. The test of the catalytic activity of the VPO sample were performed at a pressure of 1000 mbar. However, our NEXAFS experiments were performed at a total pressure of 2 mbar to minimize the influence of the gas phase on the spectra. Thus, an on-line product gas analysis with a proton-transfer-reaction mass spectrometer (PTR-MS) was installed to verify the catalytic activity of the catalyst at this pressure. The ionization conditions are well-defined and the ionization process occurs at lower interaction energies than at a conventional electron impact mass spectrometer. The proton-transfer reactions are usually nondissociative.[30,31] This results in an almost fragmentation free ionization making this method suitable for a qualitative and quantitative analysis of volatile hydrocarbons at ppb level. The PTR-MS is not sensitive to molecules such as O_2, CO, and CO_2 due to the detection principle of chemical ionization with H_3O^+-ions, because in the case of those molecules no proton-transfer reactions occur.

The PTR-MS measurements were performed simultaneously to the X-ray absorption measurements. The response signal of the PTR-MS for $m/e = 99$ (corresponding to the protonated MA molecule) is shown in Figure 2 (solid line). The variation of the catalyst temperature from room temperature to 400 °C is indicated by the dotted line. It is clearly visible that MA could be detected when the catalyst reached the reaction temperature of 400 °C. No signal corresponding to MA could be detected when the catalyst was cooled to room temperature. A subsequent increasing of the temperature to 400 °C caused the same constant activity of the catalyst to MA. No activity without the catalyst powder was observed in our chamber. Thus, to our knowledge for the first time the catalytic activity to MA of a VPO catalyst could be shown while the surface of the same sample was simultaneously characterized.

Application of highly sensitive PTR-MS for gas phase analysis allowed us to detect small differences of the catalytic activity of different VPO catalysts. A subset of differently prepared catalysts with different MA yields was compared in their performance under in situ conditions that are present in the NEXAFS experiment and at atmospheric pressure. The comparison between those measurements validate the in situ conditions as being representative of normal kinetic experiments. The data in Table 1 indicate a reasonable relation between the

TABLE 1: Normalized Yields of a Subset of Differently Prepared VPO Catalysts and the Ratio of the Yields Obtained at 2 mbar and 1 bar[a]

sample	2 mbar	1 bar	ratio
A	1.00	1.00	1.00
B	1.17	1.41	0.83
C	3.06	4.22	0.73
D	3.21	3.29	0.98

[a]The MA yields were measured at 400 °C. At 1 bar, 1.7% *n*-butane in air was used at a GSHV of 2477 h^{-1}, whereas at 2 mbar a mixture of 1.5% *n*-butane in He and 20% oxygen was passed over 50 mg of catalyst at a flow of 17.5 sccm.

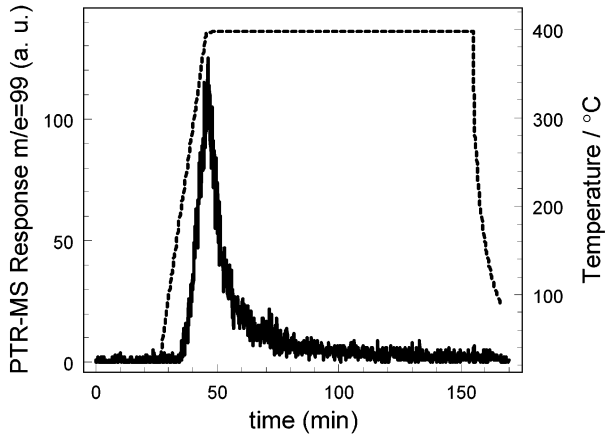

Figure 3. PTR-MS response signal (solid line) for maleic anhydride ($m/e = 99$) while the catalyst was heated from room temperature to 400 °C in pure helium at a rate of 20 °C/min.

performances if we take into account that plug flow reactors and single pellets in a flow through cell are substantially different reaction environments. This demonstrates that it is possible to deduce relevant information for the practically working catalyst by our in situ NEXAFS study.

A striking feature in Figure 2 is the high MA peak signal at the beginning of the first heating procedure. The origin of this feature was studied by heating a VPO catalyst in the XAS reaction cell in pure helium without any *n*-butane in the feed. The result of this experiment is shown in Figure 3. The same initial peak in the MA signal was detected at the beginning of the heating procedure in a butane-free atmosphere. In contrast to the case in which *n*-butane was included in the feed, no constant MA trace could be observed when the temperature was held at 400 °C for some time. The PTR-MS signal almost dropped to zero. This behavior clearly indicates that the peak is the result of desorbing MA molecules which have been attached to the catalyst surface. These adsorbed MA molecules originate from the treatment of the catalyst in the microreactor before the XAS experiment and were released under the comparatively low pressure in the XAS experiment presented in Figure 2. Thus, the decreasing MA signal is not due to a deactivation of the VPO catalyst. This initial desorption peak was much smaller when the catalyst was heated a second time to 400 °C after cooling to room temperature in between. The decreased intensity of the initial desorption peak at the beginning of the second heating cycle is due to the lower activity at 2 mbar compared to the one at 1000 mbar in the microreactor. Nevertheless, a primary release of MA still became visible. This indicates that also details of the surface state of the catalyst after the reaction at a total pressure of 2 mbar are qualitatively comparable to the ones after standard reaction conditions of 1000 mbar.

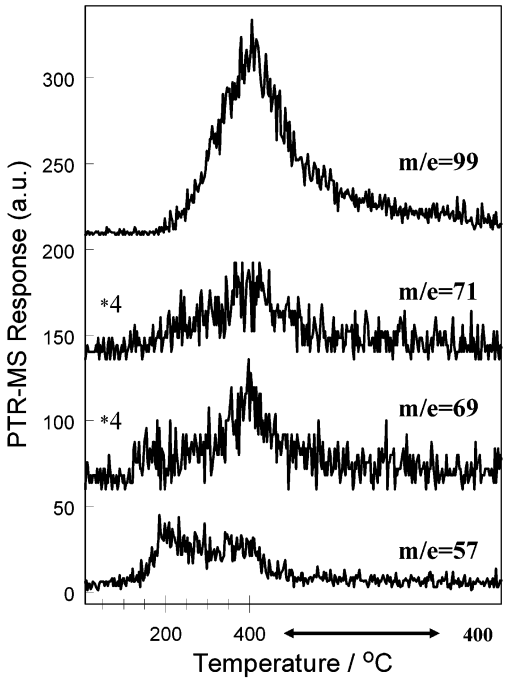

Figure 4. PTR-MS response signal for $m/e = 57$, $m/e = 69$, $m/e = 71$, and $m/e = 99$ corresponding to protonated butene, furan, dihydrofuran, and maleic anhydride molecules, respectively. The intensity for $m/e = 69$ and $m/e = 71$ is enhanced by a factor of 4. The catalyst was heated from room temperature to 400 °C in pure helium at a rate of 20 °C/min and then held at 400 °C.

In addition to MA, desorption traces of other molecules released from the surface could be detected when the catalyst was heated in He from room temperature to 400 °C. The intensity of traces belonging to $m/e = 57$, $m/e = 69$, and $m/e = 71$ versus the catalyst temperature is shown in Figure 4. The mass spectrometer signal corresponding to MA ($m/e = 99$) is also shown at the top of the figure. An assignment of the signals to the protonated molecules butene ($m/e = 57$), furan ($m/e = 69$), and dihydrofuran ($m/e = 71$), respectively, is facilitated as the detection of the molecules by PTR-MS is essentially free from fragmentation.[30,31]

It can be seen that the maximum of all of the PTR-MS signals appeared at 400 °C except for butene, where the maximum could be found around 200 °C. An additional peak appeared for the abundance of furan at approximately 150 °C. A sequential release of molecules with temperature was not observed. This would be characteristic for reaction intermediates desorbing from the surface. The data indicate an additional source for released MA molecules from the surface. The mass spectrometer signal might not stem primary from a desorption of molecules attached prior to the heating in pure He but from a synthesis of MA on the surface in the course of the heating procedure. It is possible that intermediates of the *n*-butane reaction network, perhaps butene, were also adsorbed on the surface of the catalyst during the catalytic activation and the pretest in the microreactor. These intermediates were then further transformed to furan, dihydrofuran, and finally MA on the surface. Lattice oxygen was used for the oxygen insertion steps of the reaction because no gas-phase oxygen was available during this experiment. The use of lattice oxygen for the reaction is in agreement with the literature, e.g., isotopic label experiments.[37] The surface lattice oxygens of the catalyst participate in the reaction, contrary to what happens in oxidation reactions on metals in which only the adsorbed oxygen species are directly involved.

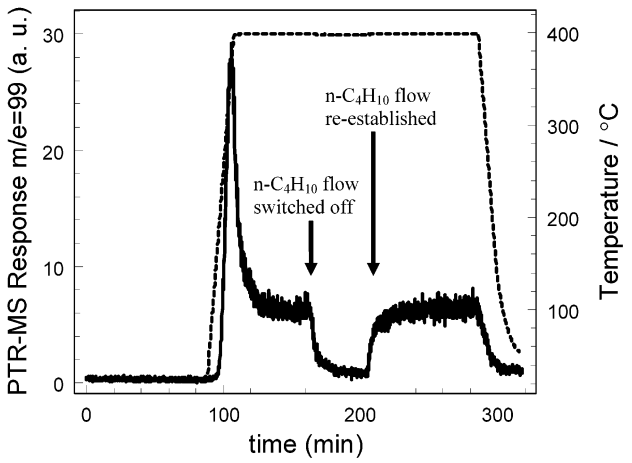

Figure 5. PTR-MS response signal (solid line) for maleic anhydride ($m/e = 99$) while the catalyst was heated from room temperature to 400 °C. At the times indicated by arrows, the feed of n-C_4H_{10}/O_2/He was replaced by a pure He flow and vice versa. The catalyst temperature was kept at 400 °C. The temperature is shown as a dashed line. The MA signal does not disappear completely in pure He flow because of residual MA in the gas inlet system of the PTR-MS.

A constant yield of MA was detected when the temperature was held at 400 °C for a long period in the case of a *n*-butane containing feed (Figure 2). A decreasing MA signal was observed when the sample was heated in pure He (Figure 3). It can be concluded that the constant level of MA in the exhaust gas of the XAS cell was due to the activity of the catalyst. Thus, XAS spectra taken under these conditions really represent the active state of the catalyst. Additionally, an experiment switching from a *n*-butane containing feed to a *n*-butane-free feed at a temperature of 400 °C was performed. The MA signal of this experiment detected by the PTR-MS is shown in Figure 5. The *n*-butane/oxygen flow was replaced with He and vice versa at the times indicated by arrows in the figure. The MA signal was rapidly vanishing without *n*-butane in the feed. The same level of MA was reestablished very soon after *n*-butane was added to the feed again.

The desorption rate at the very beginning of the heating procedure was much higher than the constant yield of the MA production at 2 mbar. This indicates that there are many more sites involved in the trapping of MA during the reaction at 1000 mbar than in the oxidation of *n*-butane to MA at 2 mbar.

To get the desired information, we analyzed the near edge X-ray absorption fine structure (NEXAFS), i.e., the strong variations of the absorption coefficient just at the absorption edge. In this report, we restrict ourselves on the absorption spectra of the vanadium site which yields detailed information about the electronic structure and also the geometric structure of the material. Furthermore, the analysis of in situ spectra is not complicated by contributions from the gas phase. The V $2p_{1/2}$ spectrum (V L_2-edge) is lifetime broadened, compared to the V $2p_{3/2}$ (V L_3-edge), due to a Coster−Kronig Auger decay into a $2p_{3/2}$ hole.[38,39] Therefore, the analysis is focused on the V L_3-edge.

In Figure 6 in situ X-ray absorption spectra of the VPO catalyst at the vanadium L_3 edge at a total pressure of 2 mbar are shown. Spectrum (a) represents the catalyst at room temperature, while spectrum (b) was taken at 400 °C. The V L_3-absorption edge corresponds to the $V2p_{3/2} \rightarrow V3d$ electronic transition. The sample showed a very detailed absorption fine structure with a number of distinct resonances that are labeled in the figure (V1−V7). Even though spectra (a) and (b) were

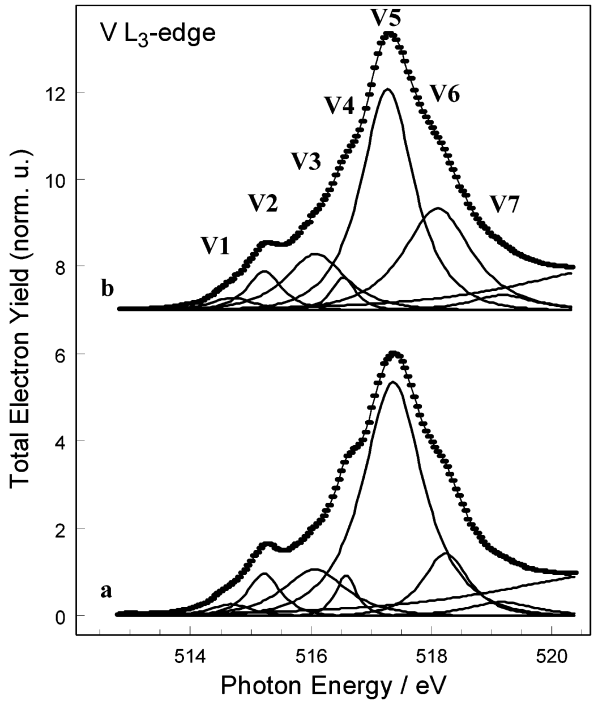

Figure 6. NEXAFS at the V L_3-edge of VPO taken at room temperature (a, lower spectrum) and at 400 °C (b, upper spectrum) in a mixture of *n*-butane/helium and oxygen at a total pressure of 2 mbar. The fit profiles used are shown and labeled V1−V7.

taken at different temperatures, they look quite similar in general. The details of the near edge absorption fine structure have been analyzed by a least-squares fit. The fitting profiles that were used are also shown in Figure 6. The resonance positions as well as the resonance intensities have been extracted by an unconstrained least-squares fit. Only the minimum number of fitting profiles that are necessary for a satisfactory fit were used in the fitting procedure without any predetermining constraints of the fitting parameters.

In the following section, the changes in the absorption spectra are analyzed when varying the catalyst temperature from room temperature to the reaction temperature of 400 °C. During the heating to 400 °C in a flow of *n*-butane and oxygen (plus helium as balance) the absorption spectrum at the vanadium L_3-edge changed significantly. The relative spectral weight of the resonance labeled V5 (compare to Figure 6) decreased as shown in Figure 7. Although there is some variation in the data, this trend is clearly visible. The MA yield detected by the PTR-MS is also shown in Figure 7 for comparison. Upon cooling the catalyst to room temperature in the reaction mixture, the intensity of resonance V5 almost recovered. At the first heating procedure ("heating") the intensity proportion of V5 is on average decreased to 86% of its initial value. The averaged values of all single spectra taken under the same conditions are presented in Figure 8. All intensities have been normalized with respect to the initial intensity of V5 before the first heating procedure. After cooling to room temperature again ("cooling"), the relative spectral intensity reached 97% of the level prior to the first heating procedure. Applying an additional heating/cooling cycle resulted in almost the same values of the intensity changes (heating 85%, cooling 96%).

A reversed behavior was observed for the spectral proportion of the resonance labeled V6 in Figure 6. These data are shown in Figure 9 normalized with respect to the initial intensity of V6 before the first heating procedure. The weight of V6 in the spectral distribution at V L_3-edge increased strongly to 161%

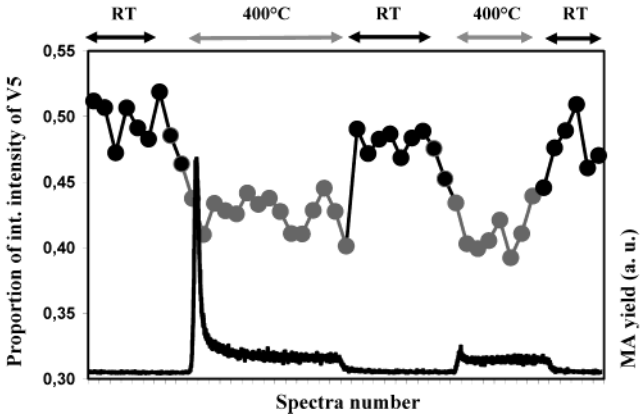

Figure 7. Proportion of the integrated intensity of resonance V5 to the spectral distribution at the V L_3-NEXAFS shown in Figure 6. Each measurement is represented by a filled circle. Measurements at the reaction temperature of 400 °C are indicated as light dots, measurements at lower temperature are shown as dark dots. The different temperature regimes are indicated by arrows at the top of the figure. The simultaneously detected catalytic activity to maleic anhydride (MA) of the material is shown at the bottom of the figure (solid line).

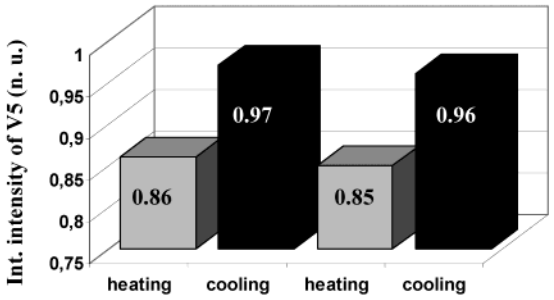

Figure 8. Normalized averaged value of the integrated intensity of resonance V5 when the catalyst was heated to 400 °C (heating) and cooled to room temperature (cooling). The initial relative intensity of V5 prior to the first heating procedure was taken as 1.

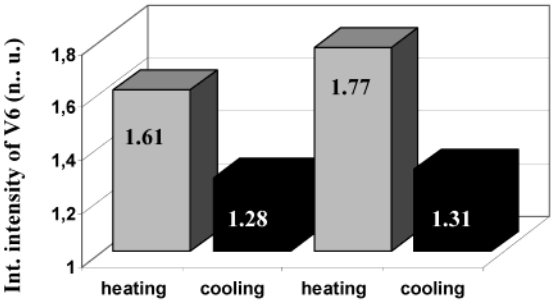

Figure 9. Normalized averaged value of the integrated intensity of resonance V6 (compare to Figure 6) when the catalyst was heated to 400 °C (heating) and cooled to room temperature (cooling). The initial relative intensity of V6 prior to the first heating procedure was taken as 1.

of its initial value at *n*-butane oxidation conditions (i.e., 400 °C, "heating"). In this case, cooling again to room temperature ("cooling") did not result exactly in the same situation as prior to the first heating procedure. Another heating/cooling cycle gave very similar results.

A downshift in photon energy for both resonances V5 and V6 was observed simultaneously with the intensity variations. The energy position of resonance V5 for every single measurement for two complete heating/cooling cycles is presented in Figure 10. The values are given relative to 517.0 eV. For comparison the MA yield detected by the PTR-MS is also shown

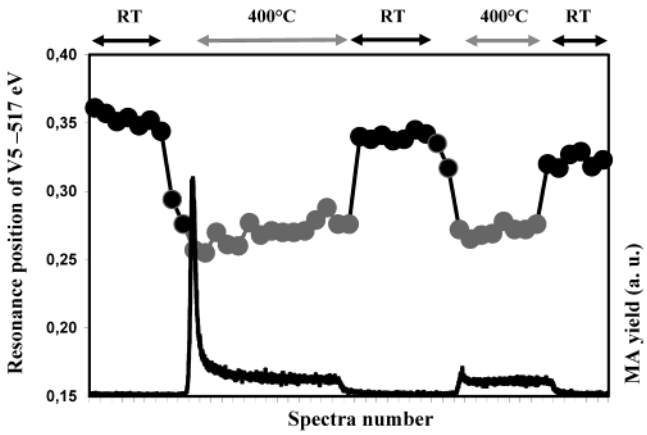

Figure 10. Photon energy position of resonance V5 (compare to Figure 6). Each measurement is represented by a filled circle. Measurements at the reaction temperature of 400 °C are indicated as light dots, and measurements at lower temperature are shown as dark dots. The different temperature regimes are indicated by arrows at the top of the figure. The simultaneously detected catalytic activity to maleic anhydride (MA) of the material is shown at the bottom of the figure (solid line). The values are given relative to 517.0 eV.

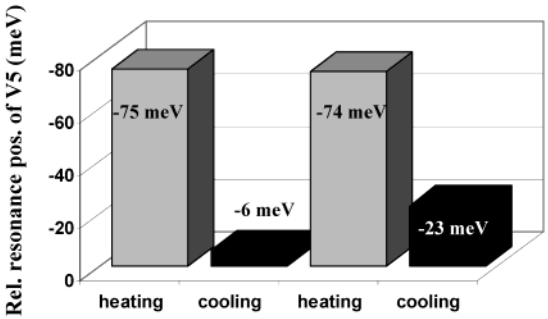

Figure 11. Normalized averaged value of the photon energy position of resonance V5 when the catalyst was heated to 400 °C (heating) and cooled to room temperature (cooling). The initial energy position of V5 prior to the first heating procedure was taken as 0.

in the figure. The resonance position of V5 was on average 75 meV lower at 400 °C than at room temperature before the heating and reached almost its initial value after cooling again to room temperature (−6 meV). The averaged values can be found in Figure 11. These changes in the NEXAFS were very reproducible during another heating/cooling cycle. The resonance position of V6 shifted more (−111 meV) than the position of V5 but also to lower photon energies when the catalyst was held at the reaction temperature of 400 °C. The energy position shift of V6 for two heating/cooling cycles is shown in Figure 12.

These observations clearly indicate that the surface structure undergoes significant rearrangements when going from the inactive state of the catalyst at room temperature to the active material. The rearrangement of the surface structure correlates with the catalytic activity of the material to maleic anhydride as shown in Figure 7 and Figure 10. The electronic structure of the catalyst observed under reaction conditions is different to the one found at room temperature. It is important to note that these structures appear to represent different equilibrium distributions, since the spectral changes were found to be reversible upon subsequent heating/cooling cycles as can be seen in Figures 7−12.

The binary vanadium oxides are known for structural rearrangements. For example, V_2O_3 undergoes a first-order transition at $T = 150$ K from an antiferromagnetic insulator phase to a

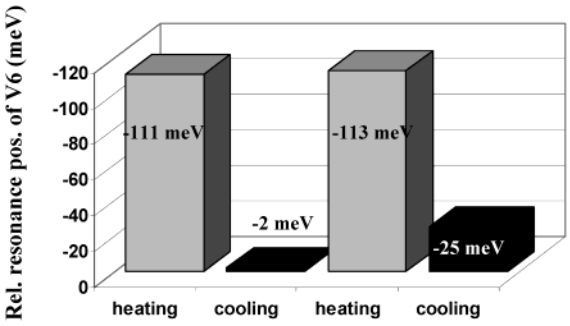

Figure 12. Normalized averaged value of the photon energy position of resonance V6 when the catalyst was heated to 400 °C (heating) and cooled to room temperature (cooling). The initial energy position of V6 prior to the first heating procedure was taken as 0.

paramagnetic metallic state above this critical temperature. V_2O_4 undergoes a first-order transition at $T = 340$ K from a nonmagnetic insulator phase at low temperature to a paramagnetic metallic state above this temperature. A comparable ability for transformations is observed in the VPO system.[14] The preparation and long term activation of the VPO catalysts have been the subject of extensive studies. It clearly appears that the surface chemistry and the bulk properties of the active catalyst change with the time of activation.[4,15,21] The evolution of the catalyst in the course of the activation process goes along with an evolution of the catalyst performance. Its surface structure is dependent on the activation conditions.

It is furthermore important to note that the observation of the reversible changes of the NEXAFS is independent of the fitting procedure and fitting profiles that are used, as long as this mathematical model is only utilized to give a description of the spectral shape of the absorption fine structures at the V L_3-edge. A physical interpretation of the fitting profiles will be discussed in the following.

A detailed interpretation of NEXAFS always requires support from theoretical calculations and simulations. Unfortunately, these are not available for the V L_3-edge for any VPO phase and in particular not for vanadyl pyrophosphate, which is often ascribed to the active phase of VPO catalysts. This is probably due to the high complexity of its geometric structure. We will therefore restrict ourselves to a more qualitative interpretation of our results.

The NEXAFS reflects the unoccupied density of states (DOS) above the Fermi level. It is site sensitive due to the high localization of the core level states. A strong hybridization between the metal 3d and O 2p states is observed for transition metal oxides in general and the binary vanadium oxides in particular; therefore, a covalent contribution to the V−O bonding is expected for VPO as well.[40−43] The V2p NEXAFS is influenced by several factors with the valence of the participating atoms, the geometric structure, and multielectron effects such as electron−electron interaction being the most important among them. The occurrence of a relative intensity change for several resonances, i.e., a redistribution of spectral weight depending on the applied conditions could mean a change in the occupation of the states or the number of this particular states. This has an impact on the chemical proportions of the surface and therefore on the catalytic performance of the material. A change in the occupation of the states means an electron transfer from energetically favored sites at room temperature to less favored at high temperature.

In this context, the intensity variation observed for the resonance V6 is interesting. The relative integrated intensity was not recovered to its initial value after the first heating procedure, but it was higher by a factor of 1.28 after the first heating/cooling cycle (compare Figure 9). This is in contrast to the intensity variation of resonance V5 that was almost completely reversible. The energy position of resonance V6 reached almost its initial value as well. It is concluded that the intensity of this resonance is influenced by the interaction of adsorbed MA or intermediates of the *n*-butane oxidation reaction. Prior to the XAS experiment, the molecules have been attached to the catalyst surface when the material was cooled in the test reactor. Most of these adsorbates have been removed during the first heating procedure as detected by the strong desorption peak shown in Figure 2. The lower coverage of the surface with these adsorbates causes the higher intensity of V6 after this procedure when the catalyst was cooled to room temperature again (Figure 9 "cooling"). The even higher intensity of V6 at *n*-butane oxidation conditions of 400 °C ("heating") follows from an even lower coverage of the surface with these specific adsorbates during the reaction. Thus, the relative intensity change of V6 may represent the modification of the electronic surface structure due to its interaction with adsorbates arising from the *n*-butane oxidation reaction cycle. The bonding of the molecules to the catalyst surface affects the occupation of the electronic states by the transfer of electrons from the adsorbate into unoccupied states and thus changes the NEXAFS. The influence of other adsorbates attached to the surface (e.g., strongly chemisorbed O_2) on the NEXAFS as shown in Figure 2 cannot be excluded, although this was not supported by our data. The high sensitivity of the PTR-MS is restricted to hydrocarbons; hence, the possible desorption of O_2 at high temperatures could not be detected.

The intensity variation of resonance V5 was almost completely reversible (Figure 8) in contrast to the findings for V6 where the relative integrated intensity did not reach its initial value after the first heating procedure (compare Figure 9). Thus, a direct link of these changes to the desorption of intermediates could not be revealed. Alternatively, the intensity ratio of the resonances may change if structural changes occur. This could mean that some resonances characterize mainly the contribution of a very thin disordered overlayer or patches of a phase different from $(VO)_2P_2O_7$ supported on a bulk of crystalline vanadyl pyrophosphate. In the course of the reaction, these contributions change and thereby indicate the participation of their related phases in the catalytic reaction.

In addition, with respect to the energy position a downward shift of the resonances V5 and V6 was observed. It is a well-known fact that the overall peak position at the vanadium $L_{2,3}$-edges is sensitive to the valence of the metal atom.[42,44,45] With decreasing oxidation state, the overall spectral weight is shifted to lower photon energies due to the different electrostatic potential at the vanadium site. The slight negative shift observed for both resonances could be interpreted as a minor reduction of the surface of a fraction of a formal oxidation state during the reaction where the surface is reoxidized when the sample is cooled in the reaction atmosphere. Major alterations of the surface vanadium oxidation state can be ruled out since the $V2p_{3/2}$ core level did not change during the heating cycles as discussed later in the text. The role of the redox and the acido−basic properties are considered as key questions for this system.[46−48] The V^{4+}/V^{5+} ratio steadily increases with activation time, thus confirming a progressive reduction of the catalyst.[15] The dynamic relative amount of V^{4+} and V^{5+} on the surface of the catalyst is clearly an important factor that determines the catalytic activity.

Structural modifications can also change the energy position of certain features in the NEXAFS as demonstrated by Eyert et al. for the binary oxide V_2O_5, that exhibits a similar local structure as vanadyl pyrophosphate.[49] The authors calculated the DOS for both the real distorted bulk structure of V_2O_5 and some hypothetical less distorted structures of the V−O octahedron. It was found that certain features of the DOS shift in energy depending on which modification of the geometric structure was assumed (approximately 2.0−2.5 eV for idealized out-of-plane displacements and 0.75−1.0 eV for idealized in-plane displacements). Eyert et al. found in general a downshift in energy when the V−O bond length was increased, i.e., a decreasing bond strength. Keeping in mind that XAS is a local method, it should be possible to conclude from the V_2O_5 system upon the VPO system because both materials show a very similar local geometric structure. In fact, the V L_3-NEXAFS of V_2O_5 and a VPO catalyst is very similar.[26] Thus, the downshift in energy of certain resonances in the course of the *n*-butane oxidation to MA observed for VPO catalysts could mean a small increase in V−O bond length like it was demonstrated theoretically by Eyert et al. in the case of V_2O_5.[49] This effect might be caused by structural modifications of the surface or by a variation in the occupation of electronic states. The variation in the occupation results in the observed intensity changes. This interpretation is comparable to Raman spectroscopy, where a downward frequency shift reflects a lengthening of the participating bond. Actually, this effect was observed by Topsøe et al. for vanadia-based catalysts that where heated in a stream of oxygen and argon.[50] Topsøe et al. explain their results with the increasing mobility of adsorbates when going from room temperature to reaction temperature. This mobility results in a transformation of these adsorbates from energetically favored O positions to other positions including nearby oxygen atoms (i.e., singly coordinated to multiple coordinated).

A tentative identification of V−O bonds in VPO that contribute mainly to the resonances V5 and V6 can be given by taking into account the theoretical results for V_2O_5. The V^{4+}-VPO-phase vanadyl pyrophosphate $(VO)_2P_2O_7$ possesses a geometric structure in which two highly distorted VO_6 octahedra are joined by the edges.[51] The structure is built up by layers parallel to the (100) plane in which pairs of octahedra are connected by PO_4 tetrahedra. The V═O bonds in the octahedra pairs are in trans position and the layers are connected by pyrophosphate groups. One can find oxygen that is singly coordinated to vanadium or phosphorus (V═O or P═O), doubly coordinated bridging oxygen (V−O−V, V−O−P, P−O−P), and triply coordinated bridging oxygen ($^{V}_{V}$>O−P). Only some peculiar oxygen atoms are active, which are involved in the redox reaction of oxygen insertion. Among these oxygen species, vanadyl oxygens V═O are frequently favored, but bridging oxygens V−O−V or V−O−P are also proposed.[47,52,53]

Recently, we suggested an empirical relationship between the resonance position at the V L_3-absorption edge of VPO and the bond length.[26] A linear dependence between the energy position of several absorption resonances and the V−O bond length of the participating atoms was found. On the basis of this finding, we proposed an assignment of certain resonances and specific V−O bonds in VPO. This finding is supported by ground-state DFT calculations of V_2O_5 which suggest that the main contributions to the DOS at the V L_3-absorption edge of V_2O_5 are ordered in the sequence of the bond lengths of the participating atoms.[49] This can be understood by the differences in the overlap of the vanadium and oxygen atoms due to the different interatomic distances.

On the basis of this model, resonance V6 of VPO should arise from states related to singly coordinated vanadyl oxygen (hybridized with V). The short vanadyl V−O bond length suggests contributions of this bonding at the high energy side of the NEXAFS although an additional influence of "e_g" states cannot be excluded (this denotation for electron orbitals is used frequently, although it is strictly valid only in O_h symmetry and not for the case of the highly distorted V−O octahedron). These functional groups may serve as sorption sites for molecules that are attached to the surface after the reaction. This is concluded by relating the intensity changes of V6 to the desorption trace of MA at different temperature treatments.

The origin of resonance V5 is less obvious. No identification of the V−O bond distance in the $(VO)_2P_2O_7$ structure can be given.[26] This resonance is a fingerprint for an additional phase at the surface of the VPO catalyst that is different to vanadyl pyrophosphate. It is most relevant to see that this resonance is a key fingerprint of the active site in the oxidation reaction as indicated by the described spectroscopic changes.

Without support from theoretical calculations and simulations of the NEXAFS, it is unfortunately not possible to attribute the experimental findings uniquely to modifications in the electronic structure of the catalyst. Thus, none of the influences on the NEXAFS discussed above can be excluded or preferred. Additionally, the influence of multielectron effects on the absorption structure is unknown at this state of the work. Nevertheless, it becomes evident from our results that the electronic structure of the surface of the active VPO catalyst under *n*-butane oxidation conditions is different from that observed for the inactive catalyst at room temperature and most likely differs also from that of vanadyl pyrophosphate. In view of the generally accepted concept of isolated active states arises the question, how a stoichiometric compound like vanadyl pyrophosphate could serve as a source for the oxygen atoms necessary for the reaction without a collapse of its geometric structure. Furthermore, the material has to serve as a source for the 14 electrons which are transferred for the reaction. The VPO catalyst material is electrically insulating at room temperature. The diverse changes of the NEXAFS suggest that it is not only one single site that is active in the *n*-butane oxidation reaction but that an ensemble of sites is involved as it is expected for such a complex reaction.

X-ray Photoelectron Spectroscopy. XPS investigations of VPO catalysts usually suffer from the charging of this highly insulating material. The apparent binding energy of the photoelectrons is shifted by this effect to higher energies. In the case of differential charging a broadening of the XPS peaks is observed. It is expected that in situ XPS decreases strongly the charging of the surface because the gas molecules that are present will be ionized by the X-ray beam and compensate the charge at the catalyst surface. Nevertheless, there was still a surface charging observed in our experiments at room temperature despite the presence of *n*-butane, oxygen, and helium at a total pressure of 2 mbar. The apparent binding energy of the O1s XPS peak is shown in Figure 13. At room temperature, the O1s peak position was found to be 545.7 eV. The peak position continually shifted to lower energies when the catalyst was heated. The O1s peak position of an uncharged surface (531.0 eV) was obtained when a temperature of approximately 250 °C was reached. The XPS peak position did not change anymore when the temperature was increased further to 400 °C. The O1s and V2$p_{3/2}$ peaks shifted in the same way so that the binding energy difference between the these peaks of 14.3 eV was conserved.

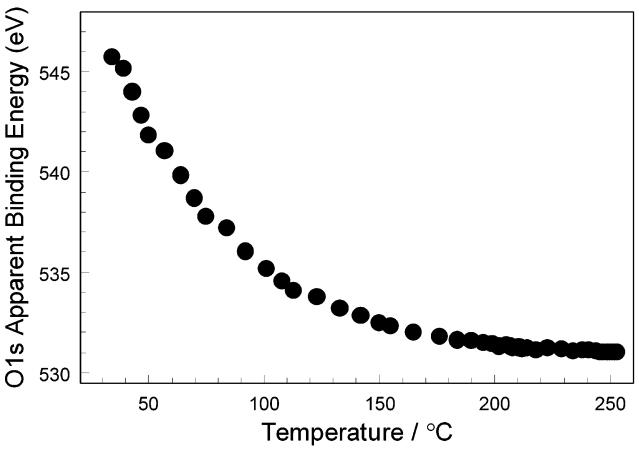

Figure 13. Apparent binding energy of the O1s peak detected by in situ XPS. The catalyst was heated from room temperature to 250 °C in a mixture of *n*-butane/helium and oxygen at a total pressure of 2 mbar.

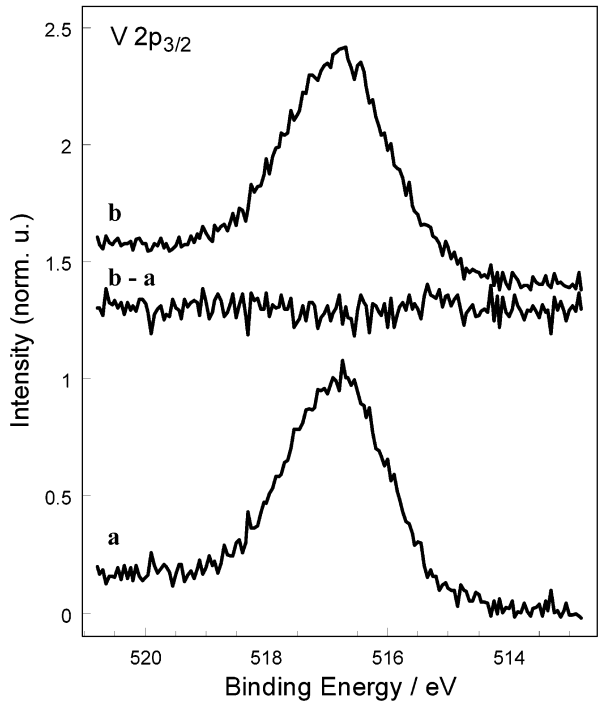

Figure 14. Vanadium $2p_{3/2}$ photoelectron peak of VPO taken at 250 °C (a, lower spectrum) and at 400 °C (b, upper spectrum) in a mixture of *n*-butane/helium and oxygen at a total pressure of 2 mbar. The photon energy was 720 eV. The spectra were normalized to the same peak height. The difference spectrum (b−a) is shown, too.

This observation means that the electric conductivity of the catalyst surface is drastically increased under reaction conditions compared to the state of the material at room temperature. The local electric conductivity is important because in the course of the *n*-butane oxidation reaction to MA 14 electrons have to be transferred.[9] The increase of the electric conductivity is completed at 250 °C. No significant yield of MA was observed at this temperature. Thus, the onset of the catalytic activity is not directly caused by the change of the surface electric conductivity.

A comparison of the $V2p_{3/2}$ photoelectron spectra taken at a temperature of 250 °C (a, lower spectrum) and taken at the *n*-butane oxidation reaction temperature of 400 °C (b, upper spectrum) is shown in Figure 14. The material is inactive for the oxidation reaction to MA at 250 °C but the charging of the surface has already completely decreased to zero (compare to Figure 13). No change of the $V2p_{3/2}$ peak was observed. The difference spectrum (b−a) is shown in Figure 14, too. XPS probes the occupied core levels of the material in contrast to X-ray absorption spectroscopy which probes the unoccupied density of states. The dynamic rearrangements observed by XAS do not influence significantly the $V2p_{3/2}$ core level which is the initial state for the $V2p_{3/2} \rightarrow V3d$ electron transition in the course of the X-ray absorption process. XPS showed a constant $V2p_{3/2}$ ground state and therefore only final state effects cause the change in the V L_3−NEXAFS of VPO under reaction conditions. The binding energy difference between the O1s and the $V2p_{3/2}$ peak is conserved as well as the shape of the $V2p_{3/2}$ peak. A constant energy separation of 14.3 eV was found between these two peaks. Thus, no hint for a major oxidation state variation in the course of the catalytic reaction at 400 °C could be observed. Minor changes of the valence (±0.15) may be difficult to detect because of the limiting signal-to-noise ratio. This observation is in agreement with the XAS results which revealed only a slight energy shift of the V L_3-edge despite the high spectral resolution.

Conclusions

Our results stress the dynamic nature of the VPO surface structure. The results show that the catalyst surface structure depends strongly on the temperature when heated in the reaction mixture of *n*-butane and oxygen. The dynamic nature of the catalyst surface is revealed by the temperature dependence of the V L_3-edge NEXAFS that represents various surface functional groups. A variation of the relative integrated intensity of specific resonances and their energy position was observed and these changes are related to the activity to maleic anhydride of the catalyst. The variation of the spectral shape indicates the presence of structural changes of the catalyst surface. One type of functional group predominates at room temperature, whereas other groups dominate at higher temperatures. It is interesting that these dynamic changes should result in a temperature dependence for the active sites involved in the catalyst, and that this behavior may influence the apparent activation energy as concluded for vanadia based DeNOx catalyst by Topsøe et al.[50] It is noteworthy that such dynamic effects would then be expected to dominate in the intrinsically more active catalysts.

It is unlikely that solely a stoichiometric bulk phase such as vanadyl pyrophosphate could facilitate all this reversible structural changes. Furthermore, the V L_3−NEXAFS possibly do not match with the pure $(VO)_2P_2O_7$ bulk phase.[26] Our results suggest the dynamic interaction of different phases on the active surface on a core of vanadyl pyrophosphate as already postulated by Hodnett.[54] In this model the active oxygen for the selective oxidation reaction does not belong to the core phase. The active surface layers might comprise different VPO phases or a distorted surface modification of vanadyl pyrophosphate.

The initial results of in situ XPS investigations show the transformation of the catalyst surface into an electrically conductive state at reaction temperature. The $V2p_{3/2}$ core level is not influenced by the structural rearrangements of the surface observed by XAS. The potential of in situ XPS to study VPO catalysts has been demonstrated in this work. More detailed investigations will be performed with an improved experimental setup soon.

Acknowledgment. The authors thank the BESSY staff for their continual support during the XAS measurements at the synchrotron in Berlin. The work is partly supported by SFB

546 of the Deutsche Forschungsgemeinschaft (DFG) and by the EPSRC. This work was supported in part (F.G.R. D.F.O. and M.S.) by the Director, Office of Energy Research, Office of Basic Energy Sciences, Material Science Division, of the U.S. Department of Energy under Contract No. DE-AC03-76F00098.

References and Notes

(1) Felthouse, T. R.; Burnett, J. C.; Mitchell, S. F.; Mummy, M. J. *Kirk-Othmer Encyclopedia of Chemical Technology*; Wiley: New York, 1995.
(2) Volta, J. C. *Chemistry* **2000**, *3*, 717.
(3) Centi, G., Ed. Vanadyl Pyrophosphate Catalysts. In *Catalysis Today*; Elsevier: Amsterdam, 1993; Vol. 16, Part 1.
(4) Bordes, E. *Catal. Today* **1987**, *1*, 499.
(5) Hodnett, B. K. *Catal. Today* **1987**, *1*, 527.
(6) Centi, G.; Trifiro, F.; Busca, G.; Ebner, J.; Gleaves, J. *Faraday Discuss*. **1989**, *87*, 215.
(7) Hutchings, G. J., *Appl. Catal*. **1992**, *72*, 1.
(8) Zhang-Lin, Y.; Forissier, M.; Sneeden, R. P. A.; Védrine, J. C.; Volta, J. C. *J. Catal.* **1994**, *145*, 256.
(9) Védrine, J. C. *Topics Catal.* **2000**, *11/12*, 147.
(10) Sciøtt, B.; Jørgensen, K. A.; Hoffmann, R. *J. Phys. Chem*. **1991**, *95***,** 2297.
(11) Centi, G.; Fornasari, G.; Trifiro, F. *J. Catal*. **1984**, *89*, 44.
(12) Ziolkowski, J.; Bordes, E.; Courtine, P. *J. Mol. Catal.* **1993**, *84*, 307.
(13) Wells, A. F. *Structural Inorganic Chemistry*; Clarendon: Oxford, 1975.
(14) Volta, J. C. *Catal. Today* **1996**, *32*, 29.
(15) Abon, M.; Béré, K. E.; Tuel, A.; Delichère, P. *J. Catal*. **1995**, *156*, 28.
(16) Kiely, C. J.; Burrows, A.; Hutchings, G. J.; Béré, K. E.; Volta, J. C.; Tuel, A.; and Abon, M. *Faraday Discuss.* **1996**, *105*, 103.
(17) Hutchings, G. J.; Desmartin Chomel, A.; Olier, R.; Volta, J. C. *Nature* **1994**, *368*, 41.
(18) Guliants, V. V.; Benziger, J. B.; Sundaresan, N. Y.; Wachs, I. E. *Catal. Lett*. **1995**, *32*, 379.
(19) Hutchings, G. J.; Lopez-Sanchez, J. A.; Bartley, J. K.; Webster, J. M.; Burrows, A.; Kiely, C. J.; Carley, A. F.; Rhodes, C.; Hävecker, M.; Knop-Gericke, A.; Mayer, R. W.; Schlögl, R.; Volta, J. C.; Poliakoff, M. *J. Catal.* **2002**, *208*, 197.
(20) Ebner, R.; Thompson, M. R. *Catal. Today* **1993**, *16*, 51.
(21) Guliants, V. V.; Holmes, S. A.; Benziger, J. B.; Heaney, P.; Yates, D.; Wachs, I. E. *J. Mol. Catal. A*, **2001**, *172*, 265.
(22) Coulston, G. W.; Bare, S. R.; Kung, H.; Birkeland, K.; Bethke, G. K.; Harlow, R.; Herron, N.; Lee, P. L. *Science* **1997**, *275*, 191.
(23) Gai, P. L.; Kourtakis, K., *Science* **1995**, *267*, 661.
(24) Briggs, D.; Seah, M. P., Eds.; *Practical Surface Analysis by Auger and X-ray Photoelectron Spectroscopy*; Wiley: New York, 1983.
(25) Abbate, M.; Goedkoop, J. B.; de Groot, F. M. F.; Fuggle, J. C.; Hofmann, S.; Petersen, H.; Sacchi, M. *Surf. Interface Anal.* **1992**, *18*, 65.
(26) Hävecker, M.; Knop-Gericke, A.; Mayer, R. W.; Fait, M.; Bluhm, H.; Schlögl, R. *J. Electron Spectrosc. Relat. Phenom.* **2002**, *125*, 79.
(27) Hävecker, M.; Knop-Gericke, A.; Schedel-Niedrig, Th.; Schlögl, R. *Angew. Chem.* **1998**, *110*, 2049.
(28) Hävecker, M.; Knop-Gericke, A.; Schedel-Niedrig, Th.; Schlögl, R. *Angew. Chem., Int. Ed. Engl.* **1998**, *37*, 206.
(29) Knop-Gericke, A.; Hävecker, M.; Schedel-Niedrig, Th.; Schlögl, R. *Top. Catal.* **2001**, *15*, 27.
(30) Lindinger, W.; Hansel, A.; Jordan, A.; *Öster. Phys. Ges*. **1998**, *2*, 7.
(31) Lindinger, W.; Hansel, A.; Jordan, A.; *Int. J. Mass Spectrom. Ion Proc.* **1998**, *173*, 191.
(32) Follath, R.; Senf, F. *Nucl. Instrum. Methods A* **1997**, *390*, 388.
(33) Senf, F.; Sawhney, K. J. S. *Nucl. Instrum. Methods A* **2001**, *467/468*, 466.
(34) Ma, Y.; Chen, C. T.; Meigs, G.; Randall, K.; Sette, F. *Phys. Rev. A* **1991**, *44*, 1848.
(35) Hussain, Z.; Huff, W. R. A.; Kellar, S. A.; Moler, E. J.; Heimann, P. A.; McKinney, W.; Padmore, H. A.; Fadley, C. S.; Shirley, D. A. *J. Elect. Spec. Relat. Phenom.*, **1996**, *80*, 401.
(36) Ogletree, D. F.; Bluhm, H.; Lebedev, G.; Fadley, C. S.; Hussain, Z.; Salmeron, M. *Rev. Sci. Instrum.*, **2002**, *73*, 3872.
(37) Abon, M.; Béré, K. E.; Delichère, P. *Catal. Today* **1997**, *33*, 15.
(38) Thole, B. T.; van der Laan, G.; Fuggle, J. C.; Sawatzky, G. A.; Karnatak, R. C.; Esteva, J.-M. *Phys. Rev. B* **1985**, *32*, 5107.
(39) Zaanen, J.; Sawatzky, G. A. *Phys. Rev. B* **1986**, *33*, 8074.
(40) de Groot, F. M. F.; Fuggle, J. C.; Thole, B. T.; Sawatzky, G. A. *Phys. Rev. B* **1990**, *41*, 928.
(41) de Groot, F. M. F.; Fuggle, J. C.; Thole, B. T.; Sawatzky, G. A. *Phys. Rev. B* **1990**, *42*, 5459.
(42) Abbate, M.; Pen, H.; Czyzyk, M. T.; de Groot, F. M. F.; Fuggle, J. C.; Ma, Y.; Chen, C. T.; Sette, F.; Fujimori, A.; Ueda, Y.; Kosuge, K. J. *Electron Spectrosc. Relat. Phenom.* **1993**, *62* 185.
(43) Zimmermann, R.; Claessen, R.; Reinert, F.; Steiner, P.; Hüffner, S. *J. Phys.: Condens. Matter* **1998**, *10*, 5697.
(44) Taftø, J.; Krivanek, O. L. *Phys. Rev. Lett.* **1982**, *48*, 560.
(45) Chen, J. G. *Surf. Sci. Rep.* **1997**, *30*, 1.
(46) Volta, J. C. *Top. Catal.* **2001**, *15*, 121.
(47) Abon, M.; Volta, J. C. *Appl. Catal*. **1997**, *157*, 173.
(48) Doornkamp, C.; Clement, M.; Gao, G.; Wachs, I. E.; and Ponec, V. *J. Catal.* **1999**, *185*, 415.
(49) Eyert, V.; Höck, K.-H. *Phys. Rev. B* **1998**, *57* 12727.
(50) Topsøe, N.-Y.; Anstrom, M.; Dumesic, J. A. *Catal. Lett*. **2001**, *76*, 1.
(51) Nguyen, P. T.; Hoffman, R. D.; Sleight, A. W. *Mater. Res. Bul.* **1995**, *30*, 1055.
(52) Michalakos, P. M.; Kung, M. C.; Jahan, I.; Kung, H. H. *J. Catal.* **1993**, *140*, 226.
(53) Wachs, I. E.; Jehng, J.-M.; Deo, G.; Weckhuysen, B. M.; Guliants, V. V.; Benziger, J. B.; Sundaresan, S. *J. Catal.* **1997**, *170*, 75.
(54) Hodnett, B. K. *Catal. Rev. Sci. Eng.* **1985**, *27*, 373.